World Journal of Translational Medicine

Online Submissions: http://www.wjgnet.com/esps/
bpgoffice@wjgnet.com
doi:10.5528/wjtm.v3.i1.17

World J Transl Med 2014 April 12; 3(1): 17-30
ISSN 2220-6132 (online)

REVIEW

Physics and mathematics of magnetic resonance imaging for nanomedicine: An overview

Odey Samuel Onwu, Oluwaseun Michael Dada, Omotayo Bamidele Awojoyogbe

Odey Samuel Onwu, Oluwaseun Michael Dada, Omotayo Bamidele Awojoyogbe, Department of Physics, Federal University of Technology, Minna, Niger State 920001, Nigeria
Author contributions: Onwu OS, Dada OM and Awojoyogbe OB contributed equally to the completion of the manuscript.
Correspondence to: Oluwaseun Michael Dada, Department of Physics, Federal University of Technology, P.M.B. 65, Minna, Niger State 920001, Nigeria. das_niger@yahoo.co.uk
Telephone: +234-813-8065478 Fax: +234-813-8065478
Received: October 7, 2013 Revised: February 16, 2014
Accepted: March 3, 2014
Published online: April 12, 2014

Abstract

Magnetic resonance imaging (MRI), magnetic resonance angiography (MRA) and magnetic resonance spectroscopy (MRS) are fundamental concepts used in modern medicine to improve health care. These concepts are based on the principle of nuclear magnetic resonance (NMR). Over the years, various laboratories around the world have applied different numerical techniques based on the Bloch NMR equations to solve specific problems in physics, biology, chemistry, engineering and medicine. The ultimate goal of any physician is to obtain maximum physical, biophysical, chemical and biological information on any tissue or cell under examination. This goal can be achieved by solving the Bloch NMR flow equations analytically. In this review, we present the basic principle of NMR/MRI in a way that can be easily understood by any researcher who needs an NMR concept to solve a specific medical problems. After a very brief history of the subject, a second order, non homogeneous, time-dependent differential equation derived from the Bloch NMR equation is presented. This equation has the basic intrinsic properties of MRI, MRA and MRS that can be extracted by means of classical and quantum mechanics for possible application in nanomedicine.

Key words: Bloch flow equations; Rotational diffusion; Molecular dynamics of biological fluids; Nuclear magnetic resonance diffusion equation; Rotational correlation time; Spherical harmonics; Molecular flow

Core tip: Magnetic resonance imaging is one of the most powerful methods for investigating structural and dynamics of biological matter. Based on quantum mechanical principles applied to Bloch nuclear magnetic resonance (NMR) flow equations, we aimed to apply the analytical solutions obtained from the Bloch NMR flow equations to nanomedicine. This may trigger research towards the design of nano devices that capable of delivering drugs directly to specifically targeted cells, with the possibility of very early diagnosis of diseases and treating them with powerful drugs at the pathological site alone, reducing any harmful side effects.

Onwu OS, Dada OM, Awojoyogbe OB. Physics and mathematics of magnetic resonance imaging for nanomedicine: An overview. *World J Transl Med* 2014; 3(1): 17-30 Available from: URL: http://www.wjgnet.com/2220-6132/full/v3/i1/17.htm DOI: http://dx.doi.org/10.5528/wjtm.v3.i1.17

INTRODUCTION

Nuclear magnetic resonance (NMR) is a very important analytical and experimental tool for physical, chemical and structural analysis of certain organic materials. Magnetic resonance is a branch of spectroscopy that detects the quantum-mechanical transitions induced by electromagnetic (EM) radiation in a system of discrete energy levels of electrons or nuclei placed in a static magnetic field[1,2]. NMR employs EM waves in the radio-frequency range between 900 MHz and 2 KHz. Some nuclei experience nuclear resonance, while others do not. Exhibition

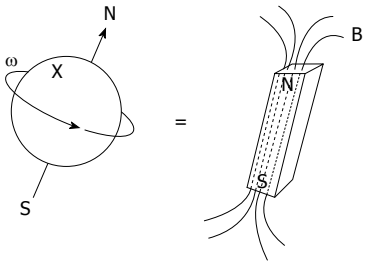

Figure 1 The charged nucleus (for example, ^{1}H) rotating with angular frequency $\omega = 2\pi\nu$ creates a magnetic field B and is equivalent to a small bar magnet whose axis is coincident with the spin rotation axis[4].

of this phenomenon is dependent on whether they possess a property called "spin"[2].

NMR is one of the most powerful methods for investigating the structure and dynamics of matter in different states of aggregation. This is due to the following features: (1) the interactions of nuclear magnetic moments are very weak compared with the thermal energy; therefore, we are dealing with para-magnetism. Moreover, the energy delivered by the radio-frequency generator are much larger compared with the strength of these internuclear couplings. That leads to the possibility of manipulating these interactions in a specific way and simplifying the spectral response; (2) the radio-frequency photons have much lower energy compared with the energy of chemical bonds. Therefore, the interaction of EM radiation with matter, particularly biomolecules, is non-ionizing; and (3) the number of radio-frequency photons with a specific frequency is very large. Hence, the phase of the associated EM wave is very well defined. The high degree of coherence of radio-frequency radiation is essential to implement NMR experiments, including magnetic resonance imaging (MRI)[3].

SPIN

Spin is a fundamental property of nature, like electrical charge or mass. Spin comes in multiples of 1/2 and can be positive (+) or negative (-). Protons, electrons and neutrons possess spins. Individual unpaired electrons, protons and neutrons each possess a spin of 1/2. In the deuterium atom (^{2}H), for example, with one unpaired electron, one unpaired proton and one unpaired neutron, the total electronic spin is equal to 1/2 and the total nuclear spin is equal to 1. Two or more particles with spins having opposite signs can pair up to eliminate the observable manifestations of spin. An example is helium, (^4_2He). In NMR, it is the unpaired nuclear spins that are important. When placed in a magnetic field of strength B, a particle with a net spin can absorb a photon, of frequency ω. The frequency of ω depends on the gyromagnetic ratio γ, of the particle [as shown in equation (1)], given by the expression:

$$\omega = \gamma B \quad (1)$$

For hydrogen nuclei, the gyromagnetic ratio γ = 42.58 MHz/T[4]. Nuclei are composed of positively charged protons and uncharged neutrons held together by nuclear forces[4,5], as shown in Figure 1.

Table 1 Properties of nuclei most useful for biological studies[5]

Nucleus	Spin quantum number (I)	Natural abundance (%)	Gyromagnetic ratio γ (10^{-7} rad/T sec)	Sensitivity[1] (% *vs* ^{1}H)	Electric quadruple moment (Q) (e.10^{24} cm^2)
^{1}H	1/2	99.9844	26.7520	100.000	-
^{2}H	1/1	0.0156	4.1067	0.965	0.00277
^{13}C	1/2	1.1080	6.7265	1.590	-
^{15}N	1/2	0.3650	-2.7108	0.104	-
^{19}F	1/2	100.0000	25.167	83.300	-
^{31}P	1/2	100.0000	10.829	6.630	-

[1]Relative sensitivity for equal number of nuclei at constant magnetic field strength.

The shell model for the nucleus tells us that nucleons, just like electrons, fill orbitals. When the number of protons or neutrons equals 2, 8, 20, 28, 50, 82 and 126, the orbitals are filled, because nucleons have spin, just like electrons do, and their spins can pair up when the orbitals are being filled and cancel out. Almost every element in the periodic table has an isotope with a non-zero nuclear spin[4,5]. NMR can only be performed on isotopes whose natural abundance is high enough to be detected; some of the nuclei that are of interest in NMR/MRI are listed in Table 1.

We have seen that $\omega = \gamma B$ and hence the energy of the radio waves needed to cause a transition between the two spin states is given by equation (2):

$$E = \eta\gamma B \quad (2)$$

When the energy of the photon matches the energy difference between the two spin states, absorption of energy occurs. In an NMR experiment, the frequency of the photon is in the radio frequency (RF) range. In NMR spectroscopy, ω is between 600 and 800 MHz for hydrogen nuclei. However, in clinical MRI, ω is typically between 15 and 80 MHz for hydrogen imaging[6] (Table 2).

To get a better understanding of how particles with spin behave under a magnetic field, we consider a proton that has a spin property. If we imagine the spin of this proton as a magnetic moment vector, causing the proton to behave like a tiny magnet with a North and South Poles. When the proton is placed in an external magnetic field, the spin vector of the particle aligns itself with the external field, just like a magnet would. There is a low energy configuration or state where the poles are aligned N-S-N-S and a high energy state N-N-S-S.

This particle can undergo a transition between the two energy states by the absorption of a photon. A particle in the lower energy state absorbs a photon and ends up in the higher energy state. The energy of this photon must exactly match the energy difference between the two states. The energy E, of a photon is related to its frequency ω, by Planck's constant ($\eta = h/2\pi$, h = 6.626 × 10^{-34} Js).

Table 2 Nuclear Spin values and gyromagnetic ratios of some nuclei[5]

Nuclei	Unpaired protons	Unpaired neutrons	Net spin	γ (MHz/T)
^{1}H	1	0	1/2	42.58
^{2}H	1	1	1/1	6.54
^{31}P	1	0	1/2	17.25
^{23}Na	1	2	3/2	11.27
^{14}N	1	1	1/1	3.08
^{13}C	0	1	1/2	10.71
^{19}F	1	0	1/2	40.08

$$E = \eta\omega \quad (3)$$

In NMR and MRI, the quantity ω is called the resonance frequency or the Larmor Frequency[6].

MRI

MRI is an imaging technique used primarily in medical settings to produce high quality images of the inside of the human body. MRI is based on the principles of NMR, a spectroscopic technique used by scientists to obtain microscopic chemical and physical information about molecules. The technique was called MRI rather than nuclear MRI because of the negative connotations associated with the word nuclear in the late 1970's. MRI started as a tomographic imaging technique; that is, it produced an image of the NMR signal in a thin slice through the human body. MRI has advanced from a tomographic imaging technique to a volume imaging technique. MRI is based on the absorption and emission of energy in the RF range of the EM spectrum[3,7].

In the past, many scientists were taught that one cannot obtain an image smaller than the wavelength of the energy being used to image it. MRI gets around this limitation by producing images based on spatial variations in the phase and frequency of the RF energy being absorbed and emitted by the imaged object.

Clinical MRI uses the magnetic properties of hydrogen and its interaction with both a large external magnetic field and radio waves to produce highly detailed images of the human body. Hydrogen has a significant magnetic moment and is the most abundant nucleus in the human body. For these reasons, we use only the hydrogen proton in routine clinical imaging[7].

To perform MRI, we first need a strong magnetic field. The field strength of the magnets used for MR is measured in units of Tesla. One (1) Tesla is equal to 10000 Gauss. The magnetic field of the earth is approximately 0.5 Gauss. Given that relationship, a 1.0 T magnet has a magnetic field approximately 20000 times stronger than that of the earth. The type of magnets used for MRI usually belongs to one of three types; permanent, resistive, and superconductive.

A permanent magnet is sometimes referred to as a vertical field magnet. These magnets are constructed of two magnets (one at each pole). The patient lies on a scanning table between these two plates[8].

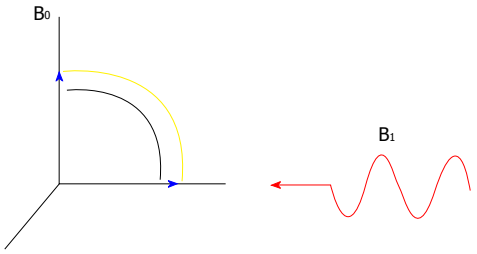

Figure 2 A 90-degree flip of the net magnetization.

The advantages of these systems are: relatively low cost, no electricity or cryogenic liquids are needed to maintain the magnetic field, their more open design may help alleviate some patient anxiety and their nearly non-existent fringe field. It should be noted that not all vertical field magnets are permanent magnets.

Resistive magnets are constructed from a coil of wire. The more turns to the coil, and the more current in the coil, the higher the magnetic field. These types of magnets are most often designed to produce a horizontal field because of their solenoid design. As previously mentioned, some vertical field systems are based on resistive magnets. The main advantages of these types of magnets are: no liquid cryogen, the ability to "turn off" the magnetic field and their relatively small fringe field.

Superconducting magnets are the most common. They are made from coils of wire (as are resistive magnets) and thus produce a horizontal field. They use liquid helium to keep the magnet wire at 4 degrees Kelvin where there is no resistance. The current flows through the wire without having to be connected to an external power source. The main advantage of superconducting magnets is their ability to attain field strengths of up to 3 Tesla for clinical imagers and up to 10 Tesla or more for small bore spectroscopy magnets[9].

CREATION OF AN MR SIGNAL

A radio wave is actually an oscillating EM field. The RF field is also referred to as the B_1 field. It is oriented perpendicular to the main magnetic field (B_0). If we apply a pulse of RF energy into the tissue at the Larmor frequency, we first find the individual spins begin to precess in phase, as will the net magnetization vector. As the RF pulse continues, some of the spins in the lower energy state absorb energy from the RF field and make a transition into the higher energy state. This has the effect of "tipping" the net magnetization toward the transverse plane. This phenomenon is illustrated in Figure 2. For the purpose of this explanation, we will assume sufficient energy is applied to produce a 90-degree flip of the net magnetization. In such an example, it is said that a 90-degree flip angle or a 90-degree pulse has been applied[10].

Oriented perpendicular to B_0 is a receiver coil. As the magnetization (now referred to as transverse magnetization, or M_{xy}) precesses through the receiver coil, a current or signal is induced in the coil. The principle behind

this signal induction is Faraday's Law of Induction. This states that if a magnetic field is moved through a conductor, a current will be produced in the conductor. If we increase the size of the magnetic field, or increase the speed with which it moves, we will increase the size of the signal (current) induced in the conductor.

To detect the signal produced in the coil, the transmitter must be turned off. When the RF pulse is discontinued, the signal in the coil begins at given amplitude (determined by the amount of magnetization precesssing in the transverse plane (Figure 2) and the precessional frequency) and fades rapidly away. This initial signal is referred to as the Free Induction Decay (FID). The signal fades as the individual spins contributing to the net magnetization lose their phase coherence, making the vector sum equal to zero. At the same time, but independently, some of the spins that had moved into the higher energy state give off their energy to their lattice and return to the lower energy state, causing the net magnetization to re-grow along the z axis. This re-growth occurs at a rate given by the tissue relaxation parameter, known as T_1[9,10].

DEFINITION OF TERMS IN NMR/MRI

Spin packets

A spin packet is a group of spins experiencing the same magnetic field strength. At any instant in time, the magnetic field caused by the spins in each spin packet can be represented by a magnetization vector; $\vec{M}$. The vector sum of the magnetization vectors from all the spin packets is the net magnetization. Adapting the conventional NMR coordinate system, the external magnetic field and the net magnetization vector at equilibrium are both along the Z axis.

T_1 relaxation time

The time constant that describes how M_z returns to its equilibrium value is called the spin lattice relaxation time (T_1). The equation governing this behavior as a function of time t after its displacement is:

$$M_z = M_o (1 - e^{-t/T_1}) \quad (4)$$

At equilibrium, the net magnetization vector lies along the direction of the applied magnetic field B_o and is called the equilibrium magnetization M_o. In this configuration, the Z component of magnetization M_z equals M_o. M_z is referred to as the longitudinal magnetization. There is no transverse (M_x or M_y) magnetization here.

Larmor frequency

The resonant frequency of a nucleus is determined by a combination of nuclear characteristics and the strength of the magnetic field. The specific relationship between resonant frequency and the field strength is an inherent characteristic of each nuclide and is generally designated as gyromagnetic ratio γ. The resonant frequency is also known as the Larmor frequency.

T_2 relaxation time

The time constant that describes the return to equilibrium of the transverse magnetization, M_{xy}, is called the spin-spin relaxation time, T_2.

$$M_{xy} = M_{xyo}\, e^{-t/T_2} \quad (5)$$

T_2 is always less than or equal to T_1. The net magnetization in the XY plane goes to zero and then the longitudinal magnetization grows in until we have M_o along Z.

Excitation

If a pulse of RF energy with a frequency corresponding to the nuclear precession rate is applied to a material, some of the energy will be absorbed by the individual nuclei. The absorption of energy by a nucleus flips its alignment away from the direction of the magnetic field. This increased energy places the nucleus in an excited state. In this excited state, the precession is now transformed into a spinning motion of the nucleus around the axis of the magnetic field[1-14].

BRIEF HISTORY ON THE DEVELOPMENT OF NMR AND MRI

The history of the development of the concept of NMR started with Felix Bloch at Harvard, and Edward Purcell at Stanford, both of whom were awarded the Nobel Prize in 1952, discovered the magnetic resonance phenomenon independently in 1946, using different instrumentation. In the period between 1950 and 1970, NMR was developed and used for chemical and physical molecular analysis. In 1971 Raymond Damadian (an Armenian-American medical practitioner and inventor of the first MR Scanning Machine) showed that the nuclear magnetic relaxation times of tissues and tumors differed, thus motivating scientists to consider magnetic resonance for the detection of disease. In 1973 the X-ray-based computerized tomography (CT) was introduced by Hounsfield. MRI was first demonstrated on small test tube samples that same year by Paul Lauterbur. He used a technique similar to that used in CT. In 1975 Richard Ernst, a Swiss physical chemist, proposed MRI using phase and frequency encoding, and the Fourier Transform. This technique is the basis of current MRI techniques. A few years later, in 1977, Raymond Damadian demonstrated MRI called field-focusing NMR. In this same year, Peter Mansfield developed the echo-planar imaging (EPI) technique. This technique was later developed to produce images at video rates (30 ms/image). Edelstein and coworkers demonstrated imaging of the body using Ernst's technique in 1980. A single image could be acquired in approximately five minutes by this technique. By 1986, imaging time was reduced to about five seconds, without sacrificing significant image quality. In the same year, the NMR microscope was developed, which allowed approximately 10m resolution on approximately one cm samples. In 1987 EPI was used to perform real-time moving imaging of a single cardiac cycle. In this same year, Charles Dumoulin perfected magnetic resonance angiography (MRA), which allowed imaging of flowing blood without the use of contrast agents.

In 1991, Richard Ernst was rewarded for his achievements in pulsed Fourier Transform NMR and MRI with the Nobel Prize in Chemistry. In 1992 functional MRI (fMRI) was developed. This technique allows the mapping of the functions of the various regions of the human brain. Five years earlier, many clinicians thought EPI's primary application was to be in real-time cardiac imaging. The development of fMRI opened up a new application for EPI in mapping the regions of the brain responsible for thought and motor control. In 1994, researchers at the State University of New York at Stony Brook and Princeton University demonstrated the imaging of hyperpolarized ^{129}Xe gas for respiration studies.

In 2003, Paul C Lauterbur of the University of Illinois and Sir Peter Mansfield of the University of Nottingham were awarded the Nobel Prize in Medicine for their discoveries concerning MRI. MRI is clearly a young, but growing science[1,3,5-16].

THE THEORY OF NMR

The appearance of NMR spectra, and consequently the molecular structure they are able to provide, arises from the discrete nature of the energy levels pertaining to a nuclear spin system. The energy levels are mainly a result of Zeeman interaction, $-\vec{\mu}\vec{B}_0$ between the static magnetic field of induction $\vec{B}_0$ and nuclear magnetic moment $\vec{\mu}$. The quantum-mechanical quantity called spin momentum, $\vec{I}$ is related to magnetic moment by $\vec{\mu} = \gamma\eta\vec{I}$, where γ is the gyromagnetic ratio and η is the Planck's constant divided by 2π.

In the absence of the magnetic nuclear, the spin states are generated. The application of a static magnetic field $\vec{B}_0$ which induces a magnetic interaction, is described by Zeeman Hamiltonian $H = -\vec{\mu}\vec{B}_0$. Taking the magnetic field orientation to be along the z-direction we get:

$$H = -\gamma\eta B_0 I_z \quad (6)$$

The Eigen values E_m of this Hamiltonian can be evaluated from the Schrodinger equation

$$H|m\rangle = -\gamma\eta B_0 m|m\rangle \quad (7)$$

where $|m\rangle$ is the Eigen state corresponding to the Eigen value $E_m = -\gamma\eta B_0 m$. The magnetic quantum number is m, where $m = l, l\text{-}1, \ldots, -l$. Therefore, the equidistant energy differences are for the single-quantum transitions $m = \pm 1$ given by[1,4,5,7]

$$\Delta E = \eta\omega_0 \quad (8)$$

where the Larmor frequency is defined as[1,4,5,7]

$$\nu_0 = \nu_L = \omega_0/2\pi$$

Another important ingredient for a magnetic resonance experiment is represented by the presence of the RF field. Only the magnetic component of the EM field, *i.e.*, $\vec{B}_1(t) = \vec{B}_{10}\cos(2\pi\nu t)$ interacts with the magnetic moment of the nuclei. The amplitude of the RF field is $\vec{B}_{10}$ and ν is the carrier frequency. This field is produced by an RF coil and leads to a perturbation Hamiltonian:

$$\vec{H}_p = -\gamma\eta\vec{B}_{10}\vec{I}\cos(2\pi\nu t) \quad (9)$$

From the time-dependent perturbation theory of quantum mechanics, it can be stated that a transition between two states $|\psi\rangle$ and $|\phi\rangle$ is allowed, provided that $\langle\psi|H_p|\phi\rangle \neq 0$. This takes place if $\nu \approx \nu_0$ (*i.e.*, the resonance condition) and the alternative magnetic field $\vec{B}_0$ is polarized perpendicular to the static magnetic field $\vec{B}_{10}$[11].

In general, NMR experiments are performed at high temperatures, employing a large number of spins. These features lead to the possibility to treat classically some aspects of the experiments. The excess of spins oriented along the static magnetic field $\vec{B}_0$ with respect to those oriented in the opposite direction results in a macroscopic nuclear magnetization $\vec{M}$, aligned along the static magnetic field, which is called the equilibrium magnetization. It can be displaced from this equilibrium by an appropriate perturbation, for instance, by an RF excitation. It is then subject to a precessional motion around $\vec{B}_0$ with the Larmor frequency ν_L. The EM perturbation that brings $\vec{M}$ into a plane perpendicular to $\vec{B}_0$ allows the observation of the Larmor precession through an electromotive force that occurs in a coil whose axis is contained in that plane. This can be done by rotation of the magnetization using a resonant 90° RF pulse. The nuclear magnetization $\vec{M}$ can be oriented antiparallel to $\vec{B}_0$ by the action of a 180° pulse. The majority of NMR experiments used pulse sequences composed of 90° and 180° RF pulses[9-18].

PULSED NMR SPECTROSCOPY

A coil of wire placed around the x-axis will provide a magnetic field along the x-axis when a direct current is passed through the coil. An alternating current will produce a magnetic field that alternates in direction. In a frame of reference rotating about the z-axis at a frequency equal to that of the alternating current, the magnetic field along the x'-axis will be constant, just as in the direct current case in the laboratory frame. This is the same as moving the coil about the rotating frame coordinate system at the Larmor Frequency. In magnetic resonance, the magnetic field created by the coil passing an alternating current at the Larmor frequency is called the B_1 magnetic field. When the alternating current through the coil is turned on and off it creates a pulsed B_1 magnetic field along the x'-axis. The spins respond to this pulse in such a way as to cause the net magnetization vector to rotate about the direction of the applied B_1 field. The rotation angle depends on the length of time τ for which the field is switched on and its magnitude, B_1[2,6,7,9].

A 90° pulse is one that rotates the magnetization vector clockwise by 90° about the x'-axis and rotates the equilibrium magnetization down to the y'-axis. In the laboratory frame, the equilibrium magnetization spirals down around the z-axis to the xy-plane. One can now see why the rotating frame of reference is helpful in describing the behavior of magnetization in response to a pulsed magnetic field. A 180° pulse will rotate the magnetization vector by 180° and rotates the equilibrium magnetization

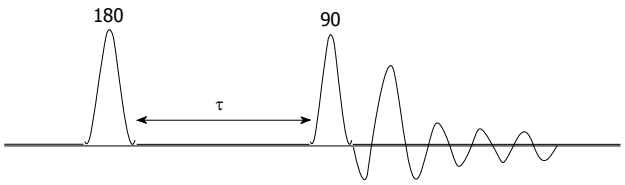

Figure 3 A series of spectra recorded with different values of τ to map out the recovery of the magnetization.

down along the z-axis.

The net magnetization at any orientation will behave according to the rotation equation. For example, a net magnetization vector along the y'-axis will end up along the y'-axis when acted upon by a 180° pulse of B_1 along the x'-axis. A net magnetization vector between x'- and y'- will end up between x' and y' after the application of 180° pulse of B_1 applied along the x'-axis[9].

Longitudinal magnetization is aligned along the field axis B_0 (that is, the z-axis) and has a finite equilibrium value of M_{0z}. M_{0z} represents the equilibrium magnetization at the start of any NMR experiment.

Transverse magnetization is perpendicular to B_0, precesses around the z-axis at the Larmor frequency and has an equilibrium value of zero[13].

$$\omega = 2\pi\nu = -\gamma B_0$$

A simple 1D NMR spectrum is obtained by a 90° pulse, followed by detection of the FID and Fourier transformation of the FID. More complicated pulse sequences allow measurement of specific parameters, 2D and multi-dimensional data.

MEASUREMENT OF T_1 RELAXATION TIMES

The inversion-recovery (IR) pulse sequence can be used to measure the T_1 relaxation times of all the resonances in a spectrum. IR pulse sequence is pictorially represented in Figure 3.

Alternatively, the zero crossing point for each peak can be used to estimate the T_1. Using the time τ_0 at which the signal I is zero:

$$\tau_0 = T_1 \ln 2 = 0.693\ T_1 \quad (10)$$

This provides a very useful spot check for the value of T_1 in any sample. We must note that the relaxation delay between subsequent scans must be set to at least 5 T_1 for experiments for good estimates of T_1.

The saturation-recovery pulse sequence starts from perfectly equal populations of α and β spin states (M_z = 0, achievable by saturation). During a subsequent waiting period t, the z-magnetization reappears in an exponential recovery until it has assumed equilibrium value M_{z0} for a very long time t:

$$M_z = M_{z0}\ (1 - e^{-t/T_1}) \quad (11)$$

An experiment of this nature does not require long recovery delays between scans; however, saturation of the spin states is not always easy[10].

PRACTICAL IMPORTANCE OF T_1 RELAXATION

Recovery delays

Any pulsed NMR experiment is repeated many times, and the scans added together to improve signal-to-noise (S/N) ratio. If the signals are not fully relaxed before each pulse/acquisition, then the signal in each scan will progressively decrease.

A recovery delay of about 5 × T_1 between subsequent scans almost completely restores M_{z0}, yielding reliable integrals. Recovery delays of about 1.4 T_1 maximizes S/N ratio, but the integrals of slowly relaxing signals will be smaller than those of the rapidly relaxing signals.

Solvent saturation

If a signal, or a whole spectrum, is irradiated continuously with RF, then the populations N_α and N_β will equalize and no signal can be observed. This can be used for selective removal of a peak, *e.g.*, a solvent peak from a spectrum. For example, in biological samples, H_2O would yield a huge signal without solvent suppression. A simple way of solvent suppression is presented by selective saturation by pre-irradiation = weak irradiation of the solvent signal during the recovery delay before the 90° pulse[10,18].

Weak interactions between the small magnetic moments of nuclear spins with the environment result in slow relaxation rates and allow the design of long and complicated pulse sequences. In contrast to optical spectroscopy, nuclear spins can access only a finite number of energy levels. This allows the accurate calculation of the outcome of pulse sequences. Transverse magnetization can be destroyed by a "pulsed field gradient": an electric current is sent through a gradient coil for a few milliseconds. This results in a wide distribution of Larmor frequencies during the gradient and, hence, averaging of the transverse magnetization vectors to zero[18].

NUCLEAR ENERGIES IN A MAGNETIC FIELD

The energy of the magnetic moment of a nuclear spin in a magnetic field is given by

$$E = -\mu B \quad (12)$$

where μ is the spin angular momentum and B is the magnetic field (in general B is a vector quantity). To conduct an NMR experiment, a sample is first placed in a static field. By convention, the direction of the static magnetic field is along the z-axis, and the magnitude of the magnetic field is given by B_0 (no longer a vector because it points only along the z-axis). In this case, the energy of a nuclear spin in an NMR magnet becomes

$$E = -\mu_z B_0 = -\gamma I_z B_0 \quad (13)$$

where γ is the gyromagnetic ratio (sometimes called the magnetogyric ratio) and I_z is the spin quantum number in the z-axis direction. The energy associated with a particu-

lar quantum number m is given as:

$$Em = -m\eta\gamma B_o \quad (14)$$

NMR transition energies are very small. These small energies translate into low sensitivity. When samples are placed into a magnetic field, a small excess of nuclei fall into the α state. This excess of spins in the α over the β states accounts for the entire net magnetization that is used in the NMR experiment. The ratio of the number of spins in the β state to those in the α state is given by a Boltzmann distribution:

$$N_\alpha/N_\beta = e^{\Delta E/(k_B T)} \quad (15)$$

where ΔE is the difference of energies of the α and β states, k_B is Boltzmann constant, and T is the absolute temperature. Higher magnetic fields produce correspondingly larger differences in spin states, leading to greater sensitivity[12,14,15].

BULK MAGNETIZATION IN AN ELECTRIC FIELD

If the bulk magnetization is along the field direction, as it is at equilibrium, then there is no torque and hence no motion. As expected, at equilibrium the system is stationary. If the system is away from equilibrium and the bulk magnetization vector is oriented other than along the z-axis, then the magnetization precesses (rotates) about the z-axis with an angular velocity given by the energy separation of the two states (γB_o). This torque will not change the length of the magnetization vector; it only varies its orientation. This orientation cannot be the only motion, since the system would never return to equilibrium. Therefore, along with the rotation, there is a relaxation of the vector to bring it back along the z-axis. Therefore the x- and y-components of the nuclear magnetization decay towards zero, and the z-component decays towards the equilibrium value (M_o)[4,10,14].

Considering bulk magnetization M that arises from all the magnetic moments in a sample, M experiences a torque when placed in a magnetic field, according to the expression given below:

$$dJ(t)/dt = M(t) \times B(t) \quad (16)$$

where $J(t)$ is the bulk spin angular momentum. The vector quantities in equation (16) are time dependent. The time-dependence of the magnetic field comes about when we apply RF pulses along the x- or y-axis. Equation (16) is essentially identical to an equation that describes the motion of a gyroscope[18-20]:

$$dL(t)/dt = r \times mg \quad (17)$$

where $L(t)$ is the gyroscope's angular momentum, r the radius from the fixed point of rotation, m is the mass, and g is gravity. Thus, a nuclear spin in a magnetic field will behave much like a gyroscope in a gravitational field. To make equation (16) useful, we use the relationship for the z-component of the magnetic moment:

$$\mu_z = \gamma I_z = \gamma\eta m \quad (18)$$

Then multiply each side by γ to yield

$$dM(t)/dt = M(t) \times \gamma B(t) \quad (19)$$

Equation (19) is the basis of the Bloch equations[18-20].

BLOCH EQUATIONS

In 1946 Felix Bloch formulated a set of equations that describe the behavior of nuclear spin in a magnetic field under the influence of RF pulses. He modified equation (19), given above, to account for the observation that nuclear spins "relax" to equilibrium values following the application of RF pulses. Bloch assumed they relax along the z-axis and in the x-y plane at different rates, but following first order kinetics. These rates are designated $1/T_1$ and $1/T_2$ for the z-axis and x-y plane, respectively. T_1 is called spin-lattice relaxation and T_2 the spin-spin relaxation. With the addition of relaxation, equation (19) becomes:

$$dM(t)/dt = M(t) \times \gamma B(t) - R\,[M(t) - M_o] \quad (20)$$

where R is the "relaxation matrix". Equation (20) can best be explained by considering each of its components:

$$dM_z(t)/dt = \gamma[M_x(t)\,B_y(t) \times M_y(t)\,B_x(t)] - [M_z(t) - M_o]/T_1$$
$$dM_x(t)/dt = \gamma[M_y(t)\,B_z(t) \times M_z(t)\,B_y(t)] - M_x(t)/T_2$$
$$dM_y(t)/dt = \gamma[M_z(t)\,B_x(t) \times M_x(t)\,B_z(t)] - M_y(t)/T_2 \quad (21)$$

The terms in equation (21) that do not involve either T_1 or T_2 are the result of the cross product in equation (20). Equation (21) describes the motion of magnetization in the "laboratory frame", an ordinary coordinate is stationary. Mathematically, the laboratory frame is not the simplest coordinate system, because the magnetization is moving at a frequency $\omega_0 = \gamma B_o$ in the x-y (transverse) plane. A simpler coordinate system is the "rotating frame", in which the x-y plane rotates around the z-axis at a frequency $\Omega = -\gamma B_o$. In the rotating frame, magnetization "on resonance" does not precess in the transverse plane. The transformation of equation (21) to the rotating frame is achieved by replacing each B_z (defined as B_o) by Ω/λ:

$$dM_z(t)/dt = \gamma\,[M_x(t)\,B_y^r(t) - M_y(t)\,B_x^r(t)] - [M_z(t) - M_o]/T_1$$
$$dM_x(t)/dt = -\Omega\,M_y(t) - \gamma\,M_z(t)\,B_y^r(t) - M_x(t)/T_2$$
$$dM_y(t)/dt = \gamma\,M_z(t)\,B_x^r(t) + \Omega\,M_x(t) - M_y(t)/T_2 \quad (22)$$

In equation (22), the components of B have been written with r superscripts to denote that it is a rotating frame[17-23].

PHYSICAL INTERPRETATION OF BLOCH EQUATIONS

We shall examine the behavior of equation (22) under two different limiting conditions, the effect of a short *RF* pulse and free precession. The RF pulse will be assumed to be very short compared to either relaxation times T_1 and T_2, as well as the angular frequency Ω. This assumption is valid for many typical pulsed NMR experiments, in which the pulse lengths can be as short as 5 μs. If the

RF pulse is applied along the x-axis, these conditions will allow us to neglect terms in equation (22) that contain T_1, T_2, Ω, and B_y.

$$dM_z/dt = -M_y(t)\,\gamma\,B_x^r(t)$$
$$dM_x(t)/dt = 0$$
$$dM_y(t)/dt = M_z(t)\,\gamma\,B_x^r(t) \quad (23)$$

Before solving equation (23), we need to discuss the meaning of $B_x(t)$ and $B_y(t)$. We can recall that B_o is the static magnetic field strength oriented along the z-axis. $B_x(t)$ and $B_y(t)$ are magnetic fields oriented along the x- and y-axes that are generated by rf pulses. By analogy to $\omega_0 = \gamma B_o$ defining the frequency of the NMR transitions in the static magnetic field, we can see that the terms $\gamma B_x(t)$ and $\gamma B_y(t)$ are frequencies of the magnetization rotating around the x- or y-axis. Thus, applying these frequencies for different periods of time will allow for different degrees of rotation around the x- or y-axis. If we introduce a frequency of rotation about the x-axis as $\omega_x = \gamma B_x(t)$, solutions to equation (23) can now be given as:

$$M_z(t) = M_o\cos(\omega_x t)$$
$$M_x(t) = 0$$
$$M_y(t) = M_o\sin(\omega_x t) \quad (24)$$

Finally, if we let $\theta = \omega_x t$ be the pulse angle, equation (24) shows that application of a magnetic field (RF pulse) along the x-axis causes the magnetization that was originally along the z-axis to rotate toward the y-axis by an angle θ. Note that when $\theta = 0$, $M_z(t) = M_o$ and $M_Y(t) = 0$ (all the magnetization is still pointing along the z-axis). When $\theta = 90°$, $M_Y(t) = M_o$ and $M_z(t) = 0$ (all the magnetization is still pointing along the y-axis). These have described the effects of a simple RF pulse. The second limiting condition for equation (22) is free precession in the absence of any applied pulse. In that case, B_x and B_y are both equal to zero, and equation (22) becomes:

$$dM_z(t)/\mathrm{d}t = -[M_z(t) - M_o]/T_1$$
$$dM_x(t)/\mathrm{d}t = -\Omega\,M_y(t) - M_x(t)/T_2$$
$$dM_y(t)/\mathrm{d}t = -\Omega M_x(t) - M_y(t)/T_2 \quad (25)$$

The solutions to equation (25) can be given as:

$$M_z(t) = M_o\,(1 - e^{-t/T_1})$$
$$M_x(t) = M_o\cos(\Omega\,t)\,e^{-t/T_2}$$
$$M_y(t) = M_o\sin(\Omega\,t)\,e^{t/T_2} \quad (26)$$

Equation (26) describes magnetization precessing in the x-y plane at a frequency Ω, while it is relaxing along the z-axis at a rate of $1/T_1$ and relaxing in the x-y plane at a rate $1/T_2$[17-19,21,24].

THE GENERAL BLOCH NMR FLOW EQUATION

The Bloch NMR flow equations can be written as[25,26]:

$$\partial M_x/\partial t + v\,\partial M_x/\partial x = -M_x/T_2 \quad (27)$$
$$\partial M_y/\partial t + v\,\partial M_y/\partial x = \gamma M_z B_1(x) - M_y/T_2 \quad (28)$$
$$\partial M_z/\partial t + v\,\partial M_z/\partial x = -\gamma\,M_z\,B_1(x) + (M_o - M_z)/T_1 \quad (29)$$

From equation (28 and 29), we have

$$v^2\frac{\partial M_y}{\partial x^2} + 2v\frac{\partial^2 M_y}{\partial x\partial t} + v\left(\frac{1}{T_1}+\frac{1}{T_2}\right)\frac{\partial M_y}{\partial x} + \left(\frac{1}{T_1}+\frac{1}{T_2}\right)\frac{\partial M_y}{\partial t}$$
$$+\frac{\partial^2 M_y}{\partial t^2} + \left[\frac{1}{T_1T_1} + \gamma^2 B_1^2(x,t)\right]M_y = \frac{\gamma\,B_1(x,t)\,M_o}{T_1} \quad (30)$$

Equation (30) is a general second order, non-homogeneous, time dependent differential equation that can be applied to any fluid flow problem. At any given time t, we can obtain information about the system, provided that appropriate boundary conditions are applied. From equation (30), we can obtain the diffusion equation, the wave equation, telephone and telegraph equations, Schrödinger's equation, Legendre's equation, *etc.*, and solve them in terms of NMR parameters by the application of appropriate initial or boundary conditions. Hence, we can obtain very important information about the dynamics of the system. It should be noted, however, that the term $F_o\gamma B_1(x, t)$ is the forcing function ($F_o = M_o/T_1$). If the function is zero, we have a freely vibrating system; otherwise, the system is undergoing a forced vibration.

NMR DIFFUSION EQUATION

A diffusion equation can easily be obtained from equation (30) if we assume that the NMR wave is a plane wave such that:

$$M_y(x, t) = A\,e^{\mu x + \eta t} \quad (31)$$

subject to the following MRI experimental conditions:

$$\gamma^2 B_1^2(x, t) << 1/(T_1\,T_2) \quad (32)$$

where μ and η are dependent on the NMR parameters. Taking

$$\eta^2 = T_g \text{ and } 2\eta = T_0 \quad (33)$$

Equation (30) becomes

$$v^2\,\partial^2 M_y/\partial x^2 + T_0\,\partial M_y/\partial t = F_o\gamma\,B_1(x, t) \quad (34)$$

If we write

$$D = -v^2/T_0$$
$$v = (-D\,T_0)^{1/2} \quad (35)$$

Then equation (34) becomes

$$\partial M_y/\partial t = D\,\partial^2 M_y/\partial x^2 + F_o/T_0\,\gamma B_1(x, t) \quad (36a)$$

Equation (36a) can be written in generalized co-ordinates as:

$$\partial M_y/\partial t = D\nabla^2 M_y + F_o/T_0\,\gamma B_1(t) \quad (36b)$$

If D represents the diffusion coefficient, then Equation (36) is the equation of diffusion of magnetization as the nuclear spins move. The function $F_o/T_0\gamma B_1(x, t)$ is the forcing function, which shows that application of the RF B_1 field has an influence on the diffusion of magnetization within a voxel. It is interesting to note that the dimension of equation (35) exactly matches that of the diffusion coefficient.

Equation (36) is only applicable when D is non-directional. That is, we have a constant diffusion coefficient (isotropic medium). Equation (36) can be considered for

restricted diffusion in various geometries[25,26]. This model would work quite well for molecules that move very short distances over a very considerable amount of time; where

$$\Omega = T_g + \gamma^2 B_1^2(x, t);$$
$$F_o = M_o/T_1;$$
$$T_g = 1/(T_1 T_2)$$
$$\text{and } T_0 = 1/T_1 + 1/T_2 \quad (37)$$

where γ is the gyromagnetic ratio, D is the diffusion coefficient, v is the fluid velocity, T_1 is the spin lattice relaxation time, T_2 is the spin relaxation time, M_o is the equilibrium magnetization, $B_1(x, t)$ is the applied magnetic field and M_y is the transverse magnetization. Solutions to equation (36) have been discussed by applying a number of analytical methods[26], and for the present purpose it is sufficient to design the NMR system in such a way that the transverse magnetization M_y, takes the form of a plane wave.

MATHEMATICAL CONCEPT OF ROTATIONAL DIFFUSION MRI AND MOLECULAR DYNAMICS OF BIOLOGICAL FLUIDS

The random re-orientation of molecules (or larger systems) is an important process for many biophysical probes. By the equipartition theorem, larger molecules re-orient more slowly than do smaller objects and, hence, measurements of the rotational diffusion constants can give insight into the overall mass and its distribution within an object. In this study, the mathematical concept of rotational diffusion MRI and molecular dynamics of biological fluids is presented. This approach ensures the analytical solution of the Bloch NMR flow equation, which enables us to obtain the NMR transverse magnetization in terms of spherical harmonic functions and NMR relaxation parameters for measuring rotational diffusion at the molecular level.

Theoretical and experimental studies to determine rotational diffusion coefficients using Fluorescence Correlation Spectroscopy, fluorescence anisotropy, flow birefringence, dielectric spectroscopy, NMR relaxation and other biophysical methods that are sensitive to picosecond or slower rotational processes have been published earlier studies[1-12].

In this study, we have presented a new method based on the Bloch NMR flow equation to measure rotational diffusion of biological fluids. The approach ensures that analytical solutions to the Bloch NMR flow equation yield the NMR transverse magnetization in terms of spherical harmonic functions and NMR relaxation parameters. The NMR/MRI technique can generate exquisite images of the soft tissue anatomy of the human body; therefore, this method is expected to become an efficient and reliable technique for measuring rotational diffusion at the molecular level for application in nanomedicine.

We consider a tumbling molecule that can be completely described by a rotational diffusion equation where the radius is fixed ($r = R$). It would be very important to derive the diffusion system directly from equations (36). Equations (36) within a spherical cavity is given by

$$\frac{\partial M_y}{\partial t} = D[\frac{1}{r^2}\frac{\partial}{\partial r}(r^2\frac{\partial M_y}{\partial r}) + \frac{1}{r^2\sin^2\theta}\frac{\partial^2 M_y}{\partial \phi^2} + \frac{1}{r^2\sin\theta}\frac{\partial}{\partial\theta}(\sin\theta\frac{\partial M_y}{\partial\theta})] \quad (38)$$

A tumbling molecule exhibits rotational diffusion that describes the tumbling motion of the molecules. In this case, the radius is fixed ($r = R$) and equation (38) becomes the rotational diffusion equation (the radial differential terms disappear):

$$\frac{\partial M_y}{\partial t} = D_r[\frac{1}{\sin^2\theta}\frac{\partial^2 M_y}{\partial \phi^2} + \frac{1}{\sin\theta}\frac{\partial}{\partial\theta}(\sin\theta\frac{\partial M_y}{\partial\theta})] \quad (38)$$

where $D_r = D/R^2$ is the rotational diffusion coefficient and R is the fixed radius of a sphere. The parameter D is called translational diffusion coefficient. The NMR transverse magnetization M_y of the diffusing molecule which is making a tumbling motion is the general solution of equation (39) obtained by the method of separation of variables:

$$M_y(\phi, \theta, t) = A\, e^{-D_r l(l+1)t}\, Y_l^m(\phi, \theta) \quad (40)$$

Equation (40) can be related to the correlation time constant τ:

$$1/\tau_1 = D/R^2\, l(l+1) = D_r\, l(l+1) \quad (41)$$

Equation (40) becomes:

$$M_y(\phi, \theta, t) = A\, e^{-t/\tau_l}\, Y_l^m(\phi, \theta) \quad (42)$$

MOLECULAR HYDRODYNAMICS IN NMR OF PROTEINS

If we sum over all possible values of m and l, equation (42) gives

$$M_y(\phi, \theta, t) = \sum_{l,m} A\, e^{-t/\tau_l}\, Y_l^m(\phi, \theta) \quad (43)$$

The rotational correlation time τ_l, is the characteristic time constant associated with the Brownian rotation diffusion of a particle in a solution. This is the time it takes the particle to rotate by one radian and it is a function of the particle size. For globular proteins, a spherical approximation can be used and the rotational correlation time is given by equation (44)[21]

$$\tau_l = 4\pi\,\eta R^3/(3kT) \quad (44)$$

where η is the viscosity of the solvent, R is the effective hydrodynamic radius of the protein molecule, k is the Boltzmann constant and T is the temperature. From the molecular weight (MW) of the protein (M), the hydrodynamic radius can be calculated as follows:

$$R = [3M/(4\pi\,\rho\, N_a)]^{1/3} + R_w \quad (45)$$

where ρ is the average density for proteins (1.37 g/cm^3), N_a is the Avogadro's number and r_w is the hydration ra-

Table 3 Nuclear magnetic resonance determined rotational correlation time values for known monomeric NESG targets[19]

NESG target (isotope labeling)	MW (kDa)	^{15}N T_1 (ms)	^{15}N T_2 (ms)	$I = T_1/T_2$	τ_I (ns)
PsR76A (NC5)	7.2	478	128	3.734375	5.1
VfR117 (NC)	11.2	605	119	5.084034	6.3
SyR11 (NC5)	12.4	630	104	6.057692	7.1
ER541-37-162 (NC5)	15.8	729	66.5	10.96241	10.0
ER540 (NC5)	18.8	909	66.5	13.66917	11.3
SoR190 (NC)	13.8	697.5	100.9	6.912785	7.7
TR80 (NC5)	10.5	612.8	102.9	5.955296	7.0
Ubiquitin (NC)	9	441.8	144.6	3.055325	4.4
HR2873B (NC)	10.7	492	115	4.278261	5.7
B-domain (NC)	7.2	423.5	153.3	2.762557	4.05
BcR97A (NC)	13.1	705.8	80.6	8.756824	8.8
PfR193A (NC)	13.6	733.9	80.9	9.071693	9.0
MvR76 (NC)	20.2	1015	64.5	15.73643	12.2
DvR115G (NC)	10.9	608.7	115.6	5.265571	6.5
MrR110B (NC5)	11.8	707	99.2	7.127016	7.8
VpR247 (NC5)	12.5	661.2	88.3	7.488109	8.05
BcR147A (NC)	11.9	645	104	6.201923	7.2
WR73 (NC5)	21.9	1261	41.3	30.53269	13.0
NsR431C (NC5)	16.8	855.5	71.2	12.01545	10.6
StR82 (NC)	9.2	537.3	100.4	5.351594	6.6

MW: Molecular weight.

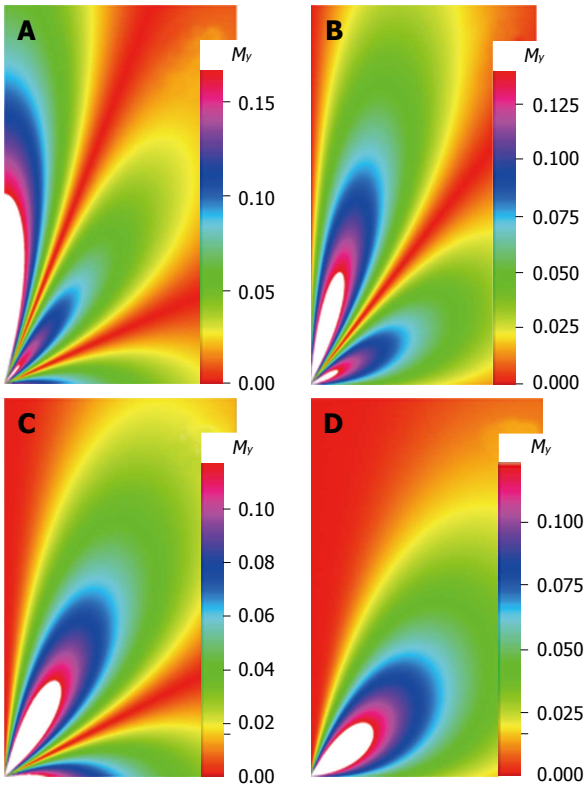

Figure 4 Image from the transverse magnetization as it varies with time, *t* = 3 ns, and the relaxation parameters τ_I = 5.1 ns, *I* = 3.734375 for (A) m = 0; (B) m = 1; (C) m = 2; (D) m = 3.

dius (1.6Å to 3.2Å). For rigid protein molecules, in the limit of slow molecular motion ($\tau_I >> 0.5$ ns) and high magnetic field (500 MHz or greater), a closed-form solution for τ_I as a function of the ratio of the longitudinal (T_1) and transverse (T_2) ^{15}N relaxation times is

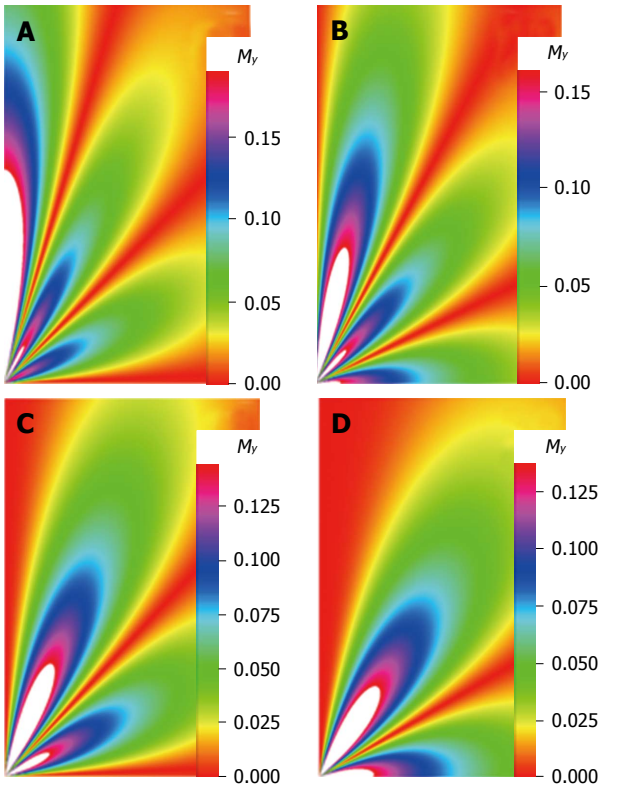

Figure 5 Image from the transverse magnetization as it varies with time, *t* = 3 ns, and the relaxation parameters τ_I = 6.3 ns, *I* = 5.084034 for (A) m = 0; (B) m = 1; (C) m = 2; (D) m = 3.

$$\tau_I = 1/(4\pi\,\omega_N)\,(6T_1/T_2 - 7)^{1/2} \qquad (46a)$$

where ω_N is the ^{15}N resonance frequency (Hz). Average ^{15}N T_1 and T_2 relaxation times for a given protein can be measured using 1D ^{15}N-edited relaxation experiments. To minimize contributions from unfolded segments, each 1D spectrum is integrated over the downfield backbone amide ^{1}H region (typically 10.5 to 8.5 ppm) and the results are used to fit an exponential decay as a function of delay time. One then computes the correlation time and compares it to a standard curve of τ_I *vs* protein MW obtained at the same temperature on a series of known monomeric proteins of varying size. The T_1/T_2 method is suitable for proteins with MW of up to MW $\approx$ 25 kDa. Accurate measurement of the diminishing ^{15}N T_2 becomes difficult for larger proteins and cross-correlated relaxation rates are measured instead[21].

The parameter I is a dimensionless constant; therefore, it may be appropriate in this study to define I as

$$I = T_1/T_2 \qquad (46b)$$

Values of rotational correlated time for some monomeric NESG (North East Structural Genomics Consortium) targets are shown in Table 1.

The density images below are obtained for the first three isotopes of Table 3, for M_0 = 1, m = 0, 1, 2, 3, and a time of 3 ns. The plots shown in Figures 4-7 are made with the assumption that the spins move across rigid spheres whose radii (= R) are in the range $\{0, 8^{1/2}\}$. Figures 4-7 give the density mapping of the transverse magnetization for specific correlation times (*i.e.*, for selected

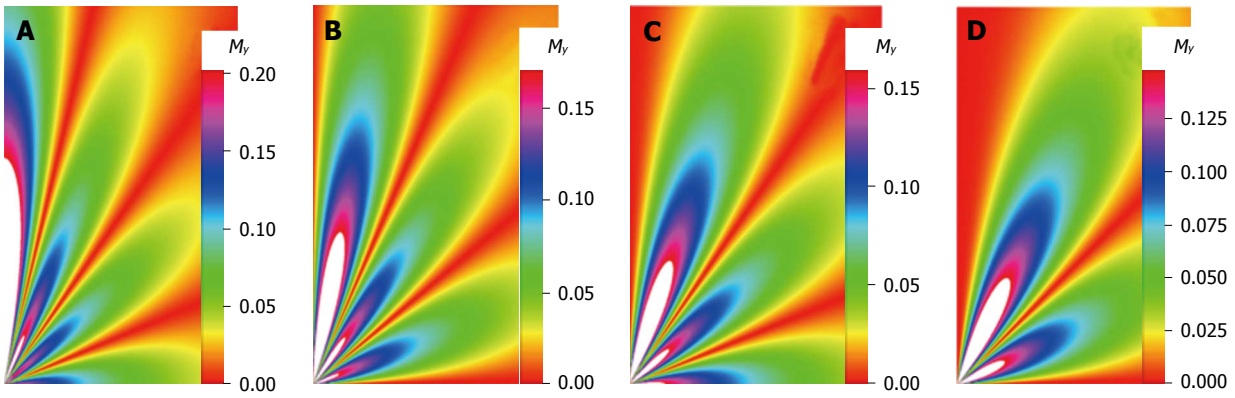

Figure 6 Image from the transverse magnetization as it varies with time, t = 3 ns, and the relaxation parameters τ_l = 7.1 ns, l = 6.057692 for (A) m = 0; (B) m = 1; (C) m = 2; (D) m = 3.

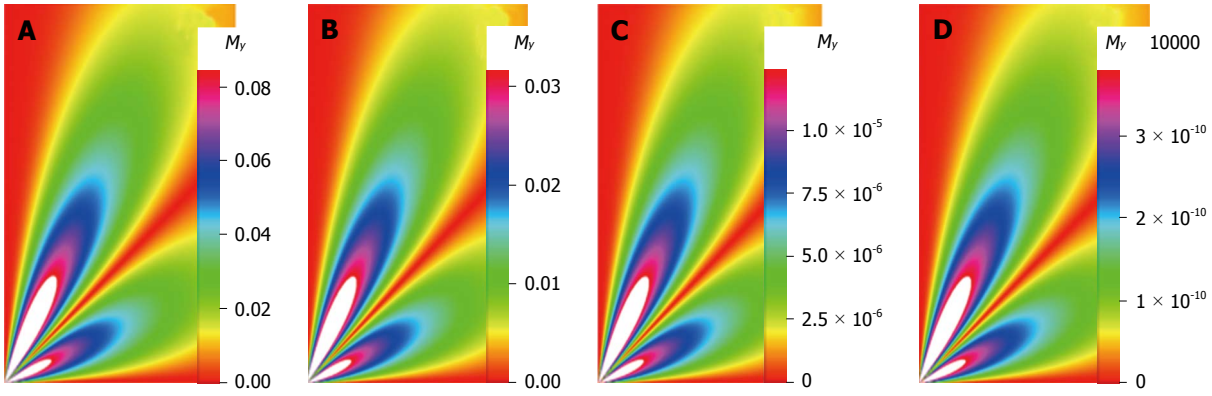

Figure 7 Image from the transverse magnetization as it varies with m = 3, and the relaxation parameters τ_l = 7.1 ns, l = 6.057692 for (A) t = 5 ns; (B) t = 10 ns; (C) t = 50 ns; (D) t = 150 ns.

NESG targets) and NMR relaxation parameters.

ROTATIONAL FRICTIONAL COEFFICIENT AND MOLECULAR NMR

When a particle moves in a fluid, either under the influence of an applied force or torque, or due to Brownian motion, it experiences frictional resistance. The proportionality between particle velocity and frictional resistance is the frictional coefficient.

It may be significant to note that the rotational diffusion coefficient D_r, can be defined from equation (39) as

$$D_r = D/R^2 = k_B T/(R^2 f_r) \quad (47)$$

where k_B is the Boltzmann's constant, f_r is the rotational frictional coefficient, R is the hydrodynamic radius of the molecule being observed and T is the absolute temperature. Equation (47) becomes discretized when the time constant is introduced:

$$1/\tau_l = k_B T/(R^2 f_r)\ l\,(l+1) \quad (48)$$

$$f_r = k_B T\,\tau_l/R^2\ l\,(l+1) \quad (49)$$

Therefore, for the NESG target PsR76A (NC5)[21], the rotational friction coefficient can easily be calculated:

$$f_r = 90.16765 \times 10^{-9}\ k_B T/R^2$$

It may be very important to note from equations (35, 39) that

$$D = -v^2/T_0 = D_r R^2 \quad (50a)$$

And

$$D_r = -v^2/(T_0 R^2) = -\omega^2/T_0 \quad (50b)$$

where

$$\omega = v/R$$

is the angular velocity. Hence, we have:

$$f_r = k_B T\,T_0/v^2 \quad (50c)$$

The angular drift velocity can be defined as

$$\Omega_d = d\omega/dT_0 = F_\omega/f_r \quad (51)$$

Equation (50b) defines the angular deviation in terms of the T_1 and T_2 relaxation parameters for rotational diffusion about a single axis

$$\omega^2 = D_r T_0 \quad (52)$$

Equation (52) describes the response of the angular drift velocity to an external torque F_ω assuming that the flow stays non-turbulent and that inertial effects can be neglected.

RELAXATION STUDIES OF DIATOMIC MOLECULES IN ROTATIONAL DIFFUSION

Rotational diffusion is a process by which the equilib-

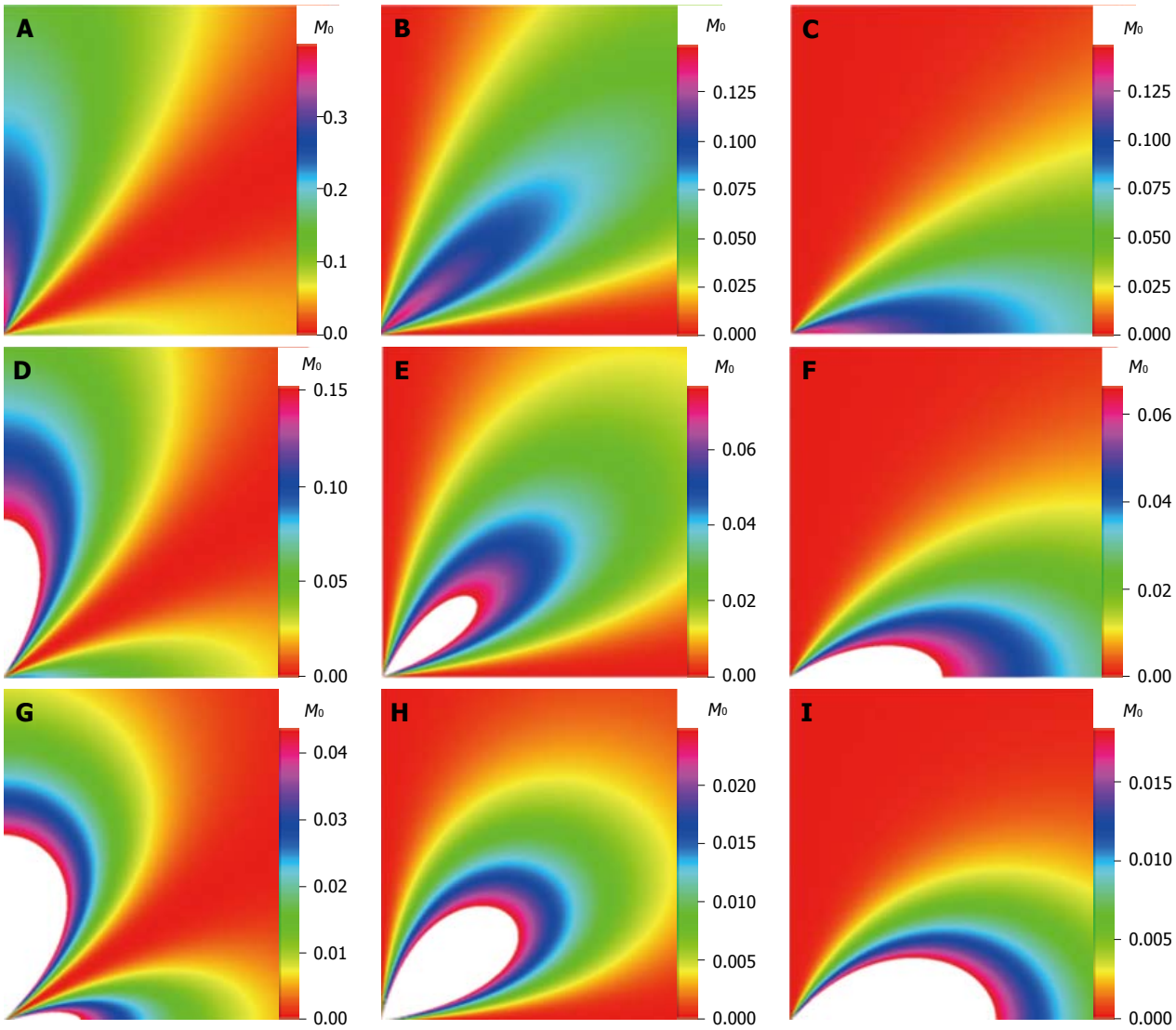

Figure 8 Density maps of M_0 using Equation (8) for l = 2 and (A) m = 0, $0 \leqslant R \leqslant 2^{1/2}$; (B) m = 1, $0 \leqslant R \leqslant 2^{1/2}$; (C) m = 2, $0 \leqslant R \leqslant 2^{1/2}$; (D) m = 0, $0 \leqslant R \leqslant 8^{1/2}$; (E) m = 1, $0 \leqslant R \leqslant 8^{1/2}$; (F) m = 2, $0 \leqslant R \leqslant 8^{1/2}$; (G) m = 0, $0 \leqslant R \leqslant 32^{1/2}$; (H) m = 1, $0 \leqslant R \leqslant 32^{1/2}$; (I) m = 2, $0 \leqslant R \leqslant 32^{1/2}$.

rium statistical distribution of the overall orientation of molecules is maintained or restored. The random re-orientation of molecules is an important process for many biophysical probes. The rotational diffusion of molecules in the presence of static magnetic and RF fields can be described by the NMR diffusion equation. The NMR diffusion equation within a spherical cavity has been described in equation (42).

The radial parameter R is constant; therefore, we may assume that $A = M_0 e^{-R}$. If we sum over all m and l, we have:

$$M_y(\phi, \theta, t) = \sum_{l,m} M_0 e^{-R_m^l} e^{-t/\tau_l} Y_l^m(\phi, \theta) \quad (53)$$

If at $t = 0$, $(\phi, \theta) = (\phi_0, \theta_0)$, we write:

$$M_y(\phi, \theta, 0) = \sum_{l,m} M_0 e^{-R_m^l} Y_l^m(\phi, \theta) = \delta[(\phi, \theta) - (\phi_0, \theta_0)] \quad (54)$$

Then, the delta function may be expanded such that:

$$\delta[(\phi, \theta) - (\phi_0, \theta_0)] = \sum_{l,m} Y_l^{m*}(\phi_0, \theta_0) Y_l^m(\phi, \theta);$$

$$M_0 e^{-R_m^l} = Y_l^{m*}(\phi_0, \theta_0) \quad (55)$$

$$M_y(\phi, \theta, t) = \sum_{l,m} Y_l^{m*}(\phi_0, \theta_0)\ Y_l^m(\phi, \theta) e^{-t/\tau_l} \quad (56)$$

For this system, the autocorrelation function may be given as:

$$G(t) = 12\pi/20\ [\mu_0/(4\pi)]^2\ \eta^2 \gamma^4/r^6$$
$$[Y_2^{m*}(\phi, \theta)\ Y_2^m(\phi, \theta) e^{-t/\tau_l}] \quad (57)$$

The angle bracket is the average over the transverse magnetization of the rotating molecules. This average is given as:

$$1/4 \int d(\phi, \theta) \int d(\phi_0, \theta_0) \sum_{l,m} Y_l^{m*}(\phi_0, \theta_0)\ Y_l^m(\phi, \theta)$$
$$Y_2^m(\phi_0, \theta_0)\ Y_2^{m*}(\phi, \theta) e^{-t/\tau_l} \quad (58)$$

If we perform the integral, we obtain[27-31]:

$$G(t) = K/3\ e^{-t/\tau_l} \quad (59)$$

where $\tau_l = R^2/(6D) = 1/(6Dr)$, and $K = 9/20\ [\mu_0/(4\pi)]^2\ \eta^2 \gamma^4/r^6$ is the second moment of interaction and r is the separation between two nuclear spins. The spectral density function is the Fourier transformation[27-31] of equation (53):

$$J(\omega) = 2/3\ [K\tau_l/(1 + \omega^2\tau_l^2)] \quad (60)$$

$$\frac{1}{T_1} = K\tau_l\left(\frac{2/3}{1 + \omega^2\tau_l^2} + \frac{8/3}{1 + 4\omega^2\tau_l^2}\right)$$

$$\frac{1}{T_2} = K\tau_l\left(1 + \frac{5/3}{1 + \omega^2\tau_l^2} + \frac{2/3}{1 + 4\omega^2\tau_l^2}\right) \quad (61)$$

MAPPING OF EQUILIBRIUM MAGNETIZATION

From equation (55), we can map M_o as a function of the radius of the rigid rotator R (which is also dependent on θ_0 and ϕ_0). At the point when RF B_1 field is just removed, M_o starts building up from its lowest value. For multi-voxel imaging, R may be changing with different tissue conditions. This may have very important influence on the changes in M_o. Figure 8 show the changes in M_o with assumed ranges for R.

CONCLUSION

We have presented the basic principle of NMR/MRI in a way that can be easily understood and that may fascinate researchers into the field of NMR/MRI. After a very brief history of the subject, a second order non-homogeneous, time dependent differential equation derived from the Bloch NMR equation was presented. Note that equation (30) uniquely assembles all the NMR, MRI, MRA and magnetic resonance spectroscopy parameters in an exciting way ready to be explored. The NMR signals as represented by equations (40-42) and Figures 4-7 are greatly influenced by the T_1 and T_2 relation times and the NMR parameter m. As l increases the motion gets faster and as m is increased, the particle's motion moves closer to orbiting the equator. This can greatly motivate further research into the use of rotational motion of nanoparticles to perform medical procedures inside the human body, noninvasively. Equations (40-42) are also the solutions for a rigidly rotating diatomic molecule. They are the angular parts of the hydrogen atom wave functions. These functions are important in many theoretical and practical applications, particularly in the computation of atomic orbital electron configurations, representation of gravitational fields, geoids, and the magnetic fields of planetary bodies and stars, and characterization of the cosmic microwave background radiation. In 3D computer graphics, spherical harmonics play a special role in a wide variety of topics including indirect lighting (ambient occlusion, global illumination, pre computed radiance transfer, *etc.*) and recognition of 3D shapes. The concept presented in this study can also be used to analyze the Earth's magnetic resonance. Application of this concept to nanomedicine will be the focus of our next investigation. Towards this goal, we derived the standard parameters of NMR relaxometry of diatomic molecules directly from the NMR diffusion equation. The advantage of this is that we are able to obtain the autocorrelation function and the spectral density function without the use of the rigorous method of probability distribution function.

REFERENCES

1 **Clare S**. Functional MRI: Methods and Applications. PhD thesis, University of Nottingham, 1997: 1-12
2 **Hornak JP**. The Basics of NMR. Available from: URL: http: //www.cis.rit.edu/htbooks/nmr/nmr-main.htm
3 **Lerner L**, Horita DA. Teaching high-resolution nuclear magnetic resonance to graduate students in biophysics. *Biophys J* 1993; **65**: 2692-2697 [PMID: 8312503 DOI: 10.1016/S0006-3495(93)81323-7]
4 **James TL**. Fundamentals of NMR. Online Textbook: Department of Pharmaceutical Chemistry, University of California, San Francisco, 1998: 1-31. Available from: URL: http: //www.biophysics.org/Portals/1/PDFs/ProfessionalDevelopment/James.T.pdf
5 **Haacke ME**, Brown RW, Thompson MR, Venkatesan R. Magnetic resonance imaging: Physical principles and sequence design. New York: John Wiley and Sons, 1999: 3-13
6 **Legault P**. Classical Description of NMR Parameters: The Bloch Equations. Online Lectures: Department de Biochimie Universite de Montreal, Montreal, 2008: 1-16. Available from: URL: http://esilrch1.esi.umontreal.ca/~syguschj/cours/BCM6200/bcm6200_NMR%20Parameters_21oct08.pdf
7 **Brix G**, Kolem H, Nitz WR, Bock M, Huppertz A, Zech CJ, Dietrich O. Basics of Magnetic Resonance Imaging and Magnetic Resonance Spectroscopy. Heidelberg: Springer Berlin, 2008: 3-167
8 **Posadas AND**, Tannus A, Panepucci CH, Crestana S. Magnetic Resonance Imaging as a non–invasive technique for investigating 3-D preferential flow occurring within stratified soil samples. *Computers and Electronics in Agriculture* 1996; **14**: 255-267 [DOI: 10.1016/0168-1699(95)00032-1]
9 **Schumacher RA**. Nuclear Magnetic Resonance. Online Publications: Carnegie Mellon University, Pittsburgh, 2009: 1-40. Available from: URL: http://www-meg.phys.cmu.edu/physics_33340/experiments/mpl_nmr.pdf
10 **Chrysikopoulos HS**. Clinical MR Imaging and Physics: A tutorial. Berlin: Springer Berlin Heidelberg, 2009: 1-31 [DOI: 10.1007/978-3-540-78023-6]
11 **Shankar R**. Principles of Quantum Mechanics. New York: Plenum Press, 1994: 265-266
12 **Slichter CP**. Principles of Magnetic Resonance. New York: Harper and Row, 1963: 1-28
13 **Abragam A**. The Principles of Nuclear Magnetism. Oxford: Clarendon Press, 1961: 1-15
14 **Ernst RR**, Bodenhausen G, Wokaun A. Principles of Nuclear Magnetic Resonance in one and two Dimensions. Oxford: Oxford University, 1990: 152-162
15 **Edison AS**. Theory and Applications of NMR Spectroscopy. Online Lecture Notes: University of Florida, Florida, 2000: 5-6. Available from: URL: http://nmrc.wsu.edu/files/ pdf/theory.pdf
16 **Cowan BP**. Nuclear Magnetic Resonance and Relaxation (First Edition). Cambridge: Cambridge University Press, 1997: 1-6
17 **Lent AH**, Hinshaw WS. An Introduction to NMR Imaging: From the Bloch Equation to the Imaging Equation. *Proc of the IEEE* 1983; **71**: 338-350 [DOI: 10.1109/PROC.1983.12592]
18 **Walker R**. Mathematics of Nuclear Magnetic Resonance Imaging. Online Publications, 2011-03-08, cited 2013-09-01; 1-8 screens. Available from: URL: http: //www.ms.uky.edu/~rwalker/research/NMR_GSC.pdf
19 **Wolff-Reichert B**. A Conceptual Tour of Pulsed NMR. Online Lecture Notes: Department of Physics and Astronomy, University of Hawaii, Hawaii, 2008: 1-8. Available from: URL: http://www.phys.hawaii.edu/~teb/phys481l/PS2A6_ConceptualTour.pdf
20 **Awojoyogbe OB**, Dada M. Mathematical Design of a Magnetic Resonance Imaging Sequence based on Bloch NMR

Flow Equations and Bessel Functions. *Chinese Journal of Magn Reson Imaging* 2013; **5**: 373-381 [DOI: 10.3969/j.issn.1674-8034.2013.05.011]
21 NMR determined Rotational correlation time. University of Buffalo Online Publication, 2011-10-13, cited 2013-09-01. Available from: URL: http: //www.nmr2.buffalo.edu/nesg.wiki/NMR_determined_Rotational_correlation_time
22 **Wang Y**. Physics of MRI. Online Lecture Notes: Polytechnic University, Brooklyn, New York, 2006: 15-25. Available from: URL: http://eeweb.poly.edu/~yao/EL5823/MRI_physics_ch12.pdf
23 **Peleg Y**, Pnini R, Zaarur E. Schaum's Outline of Theory and Problems of Quantum Mechanics. New York: McGraw-Hill Professional, 1998: 123-124
24 **Dada OM**, Awojoyogbe OB, Adesola OA, Boubaker K. Magnetic Resonance Imaging-derived Flow Parameters for the Analysis of Cardiovascular Diseases and Drug Development. *Magnetic Resonance Insights* 2013; **6**: 83-93 [DOI: 10.4137/MRI.S12195]
25 **Awojoyogbe OB**. A quantum mechanical model of the Bloch NMR flow equations for electron dynamics in fluids at the molecular level. *Phys Scr* 2007; **75**: 788 [DOI: 10.1088/0031-8949/75/6/008]
26 **Awojoyogbe OB**, Dada OM, Faromika OP, Dada OE. Mathematical Concept of the Bloch Flow Equations for General Magnetic Resonance Imaging: A Review. *Concep in Magn Reson Part A* 2011; **38A**: 85-101 [DOI: 10.1002/cmr.a.20210]
27 **Bottomley PA**, Foster TH, Argersinger RE, Pfeifer LM. A review of normal tissue hydrogen NMR relaxation times and relaxation mechanisms from 1-100 MHz: dependence on tissue type, NMR frequency, temperature, species, excision, and age. *Med Phys* 1984; **11**: 425-448 [PMID: 6482839 DOI: 10.1118/1.595535]
28 **Carneiro AAO**, Vilela GR, de Araujo DB, Baffa O. MRI relaxometry: methods and applications. *Braz J Phys* 2006; **36**: 9-15 [DOI: 10.1590/S0103-97332006000100005]
29 **Quigley MF**, Iskandar B, Quigley ME, Nicosia M, Haughton V. Cerebrospinal fluid flow in foramen magnum: temporal and spatial patterns at MR imaging in volunteers and in patients with Chiari I malformation. *Radiology* 2004; **232**: 229-236 [PMID: 15155896 DOI: 10.1148/radiol.2321030666]
30 **Compston A**, Coles A. Multiple sclerosis. *Lancet* 2002; **359**: 1221-1231 [PMID: 11955556 DOI: 10.1016/S0140-6736(02)08220-X]
31 **Miller SP**, Vigneron DB, Henry RG, Bohland MA, Ceppi-Cozzio C, Hoffman C, Newton N, Partridge JC, Ferriero DM, Barkovich AJ. Serial quantitative diffusion tensor MRI of the premature brain: development in newborns with and without injury. *J Magn Reson Imaging* 2002; **16**: 621-632 [PMID: 12451575 DOI: 10.1002/jmri.10205]

P- Reviewer: Sijens PE **S- Editor**: Song XX
L- Editor: Stewart G **E- Editor**: Liu SQ

百世登

Baishideng®

Published by **Baishideng Publishing Group Co., Limited**
Flat C, 23/F., Lucky Plaza, 315-321 Lockhart Road,
Wan Chai, Hong Kong, China
Fax: +852-31158812
Telephone: +852-58042046
E-mail: bpgoffice@wjgnet.com
http://www.wjgnet.com